APPLIED PHYSICS LETTERS **86**, 112904 (2005)

# Oxygen vacancy migration and time-dependent leakage current behavior of $Ba_{0.3}Sr_{0.7}TiO_3$ thin films

R. Meyer,[a] R. Liedtke, and R. Waser
*Institut für Werkstoffe der Elektrotechnik, RWTH Aachen, 52056 Aachen, Germany*

(Received 13 September 2004; accepted 11 January 2005; published online 7 March 2005)

The leakage current response of high-permittivity columnar-grown (Ba,Sr)$TiO_3$ thin films has been studied at elevated temperatures under dc load. We observe a thermally activated current prior to the onset of the resistance degradation with an activation energy of $E_A=1.1$ eV. A point defect model is applied to calculate the migration of electronic and ionic defects under the dc field as well as the current response of the system. We find that the peak in current is not caused by a space-charge-limited transient of oxygen vacancies, but related to a modulation of the electronic conductivity upon oxygen vacancy redistribution. Furthermore, we show that after the redistribution of electronic and ionic defects, no further increase in conductivity takes place in the simulation. © *2005 American Institute of Physics*. [DOI: 10.1063/1.1874313]

High-permittivity dielectric and ferroelectric perovskite thin films ($ABO_3$) have been studied extensively in view of their applicability as integrated buffer capacitors, high-$\kappa$ insulators in dynamic random access memories, or as a functional layer in future nonvolatile memory concepts.[1–3] One serious failure event of perovskite-type thin films is the resistance degradation under dc load. Resistance degradation denotes the increase of leakage current with time leading to a breakdown of the insulator resistance. In perovskite-type ceramics, the migration of oxygen vacancies was suggested to play a key role for resistance degradation.[4] It is likely that a similar effect is responsible for the long-term degradation of thin films.[5,6] Several authors associate imprint[7] and fatigue[8,9] with the long-term migration of oxygen vacancies. In addition, a current transient prior to the resistance degradation, also referred to as hump, was observed.[10]

The focus of this letter is to compare the dc current response of (BaSr)$TiO_3$ (BST) thin films with model simulations to elucidate the nature of this current peak prior to the resistance degradation, and the degradation mechanism itself. The current peak has been reported earlier by Zafar *et al.*,[10] and was attributed to a space-charge-limited transient of oxygen vacancies. Our simulations are based on the point defects model developed for bulk material. It is adapted to thin films and accounts for the particular boundary conditions of Schottky contacts at the Pt/BST interface. The thin film is assumed to be impurity acceptor doped with an acceptor concentration of $N_A=5\times10^{19}$ $cm^{-3}$.[8,11] A weak electronic conductivity is found, since acceptor states are mostly self-compensated by oxygen vacancies. The metal/perovskite interface is modeled by a Schottky barrier for electron holes with an energy barrier height for electrons of $\phi_b=1.3$ eV.[12,13] Image forces and low-$\kappa$ interfacial layers are neglected for simplicity. In a first simulation run, the oxygen sublattice is equilibrated with the atmosphere at processing temperatures, where oxygen exchange is expected to take place with the ambient. Then, the redistribution of defects is calculated at temperatures at which the leakage current experiment is performed assuming that the interface is oxygen impermeable. Finally, the transient redistribution of ionic and electronic defects is calculated under an external field, again with respect to blocking electrodes for oxygen. Ionic and electronic currents are monitored as a function of time and compared to experimental data.

Columnar-grown BST films, typically 130 nm thick, are deposited by chemical solution deposition (Ref. 14) on a platinized Si wafer. The Pt top electrodes of 100 nm thickness are deposited by rf magnetron sputtering and patterned by a lift-off process. The surface area of the top electrodes is 0.19 $mm^2$. Capacitors are then postannealed under a $N_2$ atmosphere at $T=600$ °C for 30 min in a rapid thermal anneal facility and rapidly cooled down to room temperature. The dc current response as a function of time for different temperatures is acquired with a Keithley 617 picoampmeter. Within the time resolution limit of 1 s of the setup and due to the presence of high leakage currents, data acquisition starts after the dielectric relaxation of the capacitor. Results are shown in Fig. 1.

In the simulation, we model a cross section of the capacitor of $L=130$ nm thickness along $x$. A finite differences approach is used to calculate the redistribution of electrons $n$, electron hole $p$, and oxygen vacancies $V_O^{\cdot\cdot}$ by diffusion and drift, as well as the inner electric field and the energy band configuration with respect to boundary conditions of a Schottky contact. For the particle flux density $j_k$ of each in-

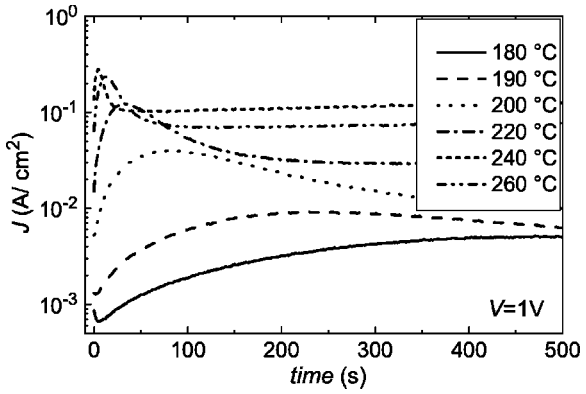


FIG. 1. Current response of a Pt/BST/Pt capacitor structure of 130 nm thickness under 1 V dc load at different temperatures. The current peak is thermally activated with 1.1 eV.

[a]Electronic mail: r.meyer@fz-juelich.de

 

dividual defect $k$, we write the Nernst–Planck equation:

$$j_k = -D_k \frac{dC_k}{dx} + \frac{z_k}{|z_k|}\mu_k C_k E,\ k \in \{n,p,V_O^{\cdot\cdot}\}. \tag{1}$$

Here, $D_k$ is the diffusivity and $\mu_k$ denotes the mobility of the respective defect. $C_k$ is the concentration and $E$ terms the inner electric field. The migration of the oxygen vacancies is thermally activated with an activation energy of 0.9–1.0 eV.[15,16] Electron and hole mobilities reveal a slight temperature dependence following a $T^{-\alpha}$ law.[17] Mobilities and diffusion coefficients are linked by the Nernst–Einstein relation.

If we assume the dielectric susceptibility $\varepsilon_r$ solely to depend on temperature, the inner electric field $E$ is given by

$$E(x) = \int_0^x \frac{\rho(\xi)}{\varepsilon_0 \varepsilon_r} d\xi. \tag{2}$$

Here, $\rho$ is the space charge, and $\varepsilon_0$ is the vacuum permittivity. Low-$\kappa$ interfacial layers and a field dependence of $\varepsilon_r$ are neglected for simplicity. The apparent space charge $\rho$ inside the film is given by

$$\rho(\xi) = -e_0(2[V_O^{\cdot\cdot}](\xi) + p(\xi) - n(\xi) - N_A). \tag{3}$$

Charges on left the and on the right electrode $\rho_{\text{electrode}}$ caused by a charge transfer between the electrode and thin film due to the Schottky contact[18] are also considered. Data for the relaxor behavior of $\varepsilon_r$ are taken from Ref. 19.

Boundary conditions at the metal/thin-film interface for electronic charge carriers, oxygen vacancies, and the electrode charges are defined as follows. For an ideal Schottky contact, the electron concentration at the electrodes $n_{x=0,L}$ is determined by the contact barrier $\phi_b$. Following Sze's textbook,[18] the surface concentrations of electrons is given by

$$n_{x=0,L} = N_C \times \exp\left(-\frac{e_0 \phi_b}{k_B T}\right). \tag{4}$$

$N_C$ is the density of states in the conduction band of the thin film and was determined by Moos *et al.*[17] for $SrTiO_3$. Similarly, the concentration of electron holes at the interface is calculated. At elevated temperatures, where the system can exchange oxygen with the atmosphere, the interface concentration of oxygen vacancies is given by the defect reaction

$$O_O^{\times} \rightleftharpoons \frac{1}{2}O_2(g) + 2e' + V_O^{\cdot\cdot}. \tag{5}$$

The boundary condition for oxygen vacancies at the interface is

$$[V_O^{\cdot\cdot}]_{x=0,L} = \frac{\kappa_{\text{red}}}{pO_2^{0.5} n_{x=0,L}^2}. \tag{6}$$

Here, $\kappa_{\text{red}}$ denotes the mass action coefficient for the reduction reaction of the oxygen sublattice.[15]

At temperatures where the leakage current experiments are performed, the metal electrodes are assumed to form a blocking contact for oxygen in the experimental time scale. The particle flux of oxygen vacancies across the metal/BST interface therefore vanishes

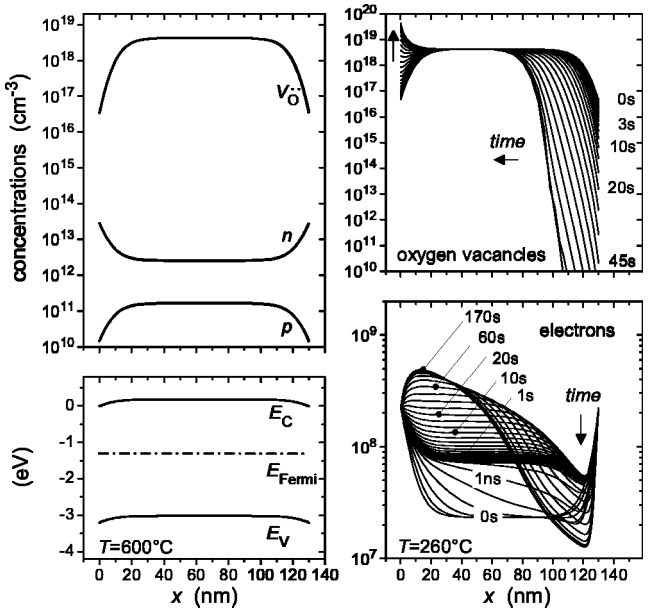


FIG. 2. (Left) Calculated electron, hole, and oxygen vacancy distribution, and energy band diagram inside the BST thin film at $T=600\,^{\circ}\text{C}$ for $pO_2=0.1$ Pa for contact barrier height of 1.3 eV. (right) Redistribution of electrons and oxygen vacancies at $T=260\,^{\circ}\text{C}$ under a dc bias voltage of $U=1$ V.

$$j_{V_O^{\cdot\cdot}}|x=0,L \equiv \text{null}. \tag{7}$$

The charges of the metal electrodes are derived from the conservation of charge with respect to the applied bias. The global electroneutrality including the electrode charges leads to:

$$\int_0^L \rho(\xi) d\xi \equiv \text{null}. \tag{8}$$

The external voltage $V_{\text{ext}}$ can be expressed as the difference of the Fermi levels $E_{\text{Fermi}}$ between the electrodes

$$e_0 V_{\text{ext}} = E_{\text{Fermi}}(x=L) - E_{\text{Fermi}}(x=0). \tag{9}$$

The Fermi energy is derived from

$$E_{\text{Fermi}}(x) = \frac{k_B T}{e_0} \ln\left(\frac{n(x)}{N_C}\right) + E_C(x), \tag{10}$$

where the bending of the conduction-band is given by the integral over the electric field in the film:

$$E_C(x) = \int_0^x E(\xi) d\xi. \tag{11}$$

The oxygen vacancy displacement current is deduced from the derivative of the charges situated on the electrodes with respect to time $\partial \rho_{\text{electrode}}/\partial t$. From the displacement current and the electronic current into the thin films, we calculate the current response which consists of electronic and displacement contribution. Details will be given elsewhere.

Figure 2 shows the defect profiles of electrons, electron holes, and oxygen vacancies for an impurity acceptor concentration of $N_A = 5 \times 10^{18}\ \text{cm}^{-3}$ after equilibration of the oxygen sublattice with the atmosphere of $pO_2 = 0.1$ Pa at 600 °C. In the core, the thin film is slightly $n$-type conductive. In the vicinity of the electrodes, holes and oxygen vacancies are depleted and an electron-enriched layer is formed

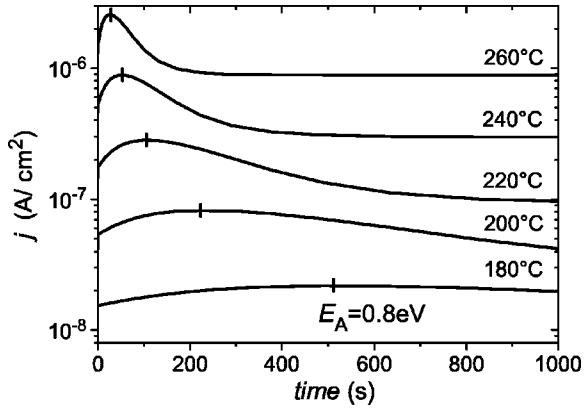


FIG. 3. Simulated current response for different temperatures. The current maximum is thermally activated with $E_A$=0.8 eV.

due to the contact potential at the Schottky interface as reported earlier by McIntyre[20] and Hwang *et al.*[21] The corresponding energy band diagram with the conduction band $E_C$, the valence band $E_V$, and the Fermi edge $E_{\mathrm{Fermi}}$ are also illustrated in Fig. 2 (left-hand side). The internal electric field, formed by the Schottky contact, is regarded as the driving force for the observed migration of the positively charges oxygen vacancies. The final state is reached within seconds under process conditions or if the film is postannealed to improve the electrical properties.[11] Although the concentration of oxygen vacancies is orders of magnitude higher than the content of electrons and holes, the film displays electronic conductivity, caused by the higher mobility of electronic species. Electron profile, internal electrical field, and band bending are strongly influenced by the oxygen vacancy profile.

The following calculations are performed after quenching the sample in the simulation down to a temperature, at which the leakage current experiment is carried out. Under an external electric field, electrons (and holes) redistribute almost instantaneously giving rise to the asymmetric electron profile shown in Fig. 2 (right-hand side). With a delay of about 1 s, a significant migration of oxygen vacancies is found as well and both oxygen vacancies and electrons accumulate at the negative electrode (here, left-hand side electrode).

During redistribution, an thermally activated increase of the leakage current is observed as illustrated in Fig. 3. This increase is not due to an additional displacement current caused by oxygen migration, but originates from a local modulation of the electron concentration in the film. Simulations performed for different temperatures display an activation energy of 0.8 eV, which is a reasonable value for oxygen vacancy migration in BST. The difference in current densities between simulation and experiment might originate from a lower effective contact potential than that assumed in the calculation. This difference can be reduced by an adjustment of $\phi_b$.

After the transient in the electronic current, migration of oxygen vacancies stops and the current response becomes time invariant. A further increase of current, which could be related to resistance degradation, does not occur. This unexpected result suggests that another mechanism, which has not been taken into account, is responsible for the resistance degradation in thin films. One possible scenario is the loss of oxygen at the positively charged electrode. Further investigations are essential to elucidate the nature of resistance degradation in thin films and to study the impact of barrier lowering by image forces, low-$\kappa$ interfacial layers, a field dependent dielectric constant $\varepsilon_r(E)$, and the presence of interface states on the leakage current response.

In conclusion, the dc current response of BST thin-film capacitors is compared to numerical calculations of the redistribution of electronic and ionic defects with respect to the boundary conditions of a Schottky barrier at the electrode/BST interface. It is shown that the current peak prior to the onset of the resistance degradation originates from a modulation of the electronic conductivity rather than a transient ionic current. The modulation in conductivity is then caused by the migration of oxygen vacancies acting as mobile donors. The suggested model cannot explain the resistance degradation, which was found experimentally. This unexpected result indicates that the key mechanism responsible for resistance degradation in thin films has not yet been taken into consideration in the model.

[1] *Nanoelectronic and Information Technology*, edited by R. Waser (Wiley-VCH, Weinheim, 2003).
[2] D. E. Kotecki, Integr. Ferroelectr. **16**, 1 (1997).
[3] T. Ueda, A. Noma, and D. Ueda, Integr. Ferroelectr. **7**, 45 (1995).
[4] R. Waser, T. Baiatu, and K.-H. Haerdtl, J. Am. Ceram. Soc. **73**, 1645 (1990).
[5] C. Basceri, S. Lash, C. Parker, S. Streiffer, A. Kingon, M. Grossmann, S. Hoffmann, M. Schumacher, R. Waser, S. Bilodean, R. Carl, P. C. Van Buskirk, and S. R. Summerfeld, Mater. Res. Soc. Symp. Proc. **493**, 9 (1998).
[6] M. Grossmann, S. Hoffmann, S. Gusowski, R. Waser, S. Streiffer, C. Basceri, C. Parker, S. Lash, and A. Kingon, Integr. Ferroelectr. **22**, 83 (1998).
[7] W. L. Wairen, D. Dimos, G. E. Pike, B. A. Tuttle, M. V. Raymond, P. Ramesh, and J. T. Evans, Appl. Phys. Lett. **67**, 866 (1995).
[8] M. Dawber and J. F. Scott, Appl. Phys. Lett. **76**, 1060 (2000).
[9] J. F. Scott and M. Dawber, Appl. Phys. Lett. **76**, 3801 (2000).
[10] S. Zafar, B. Hradsky, D. Gentile, P. Chu, R. E. Jones, and S. Gillespie, Appl. Phys. Lett. **86**, 3890 (1999).
[11] J. C. Shin, J. Park, C. S. Hwang, and H. J. Kim, J. Appl. Phys. **86**, 506 (1999).
[12] C. S. Hwang and S. H. Joo, J. Appl. Phys. **85**, 2431 (1999).
[13] G. W. Dietz, M. Schumacher, R. Waser, S. K. Streiffer, C. Basceri, and A. I. Kingon, J. Appl. Phys. **82**, 2359 (1997).
[14] S. H. U. Hasenkox and R. Waser, J. Sol-Gel Sci. Technol. **12**, 67 (1998).
[15] C.-P. Song and H.-I. Yoo, J. Am. Ceram. Soc. **83**, 773 (2000).
[16] R. Waser, J. Am. Ceram. Soc. **74**, 1934 (1991).
[17] R. Moos, W. Menesklou, and K. H. Haerdtl, Appl. Phys. A: Mater. Sci. Process. **61**, 389 (1995).
[18] S. M. Sze, *Physics of Semiconductor Devices* (Wiley, New York, 1981).
[19] R. L. U. Ellerkmann and R. Waser, Ferroelectrics **271**, 315 (2002).
[20] P. McIntyre, J. Appl. Phys. **89**, 8074 (2001).
[21] C. S. Hwang, B. T. Lee, C. S. Kang, K. H. Lee, H. J. Cho, H. Hideki, W. D. Kim, S. I. Lee, and M. Y. Lee, J. Appl. Phys. **85**, 287 (1999).